

Supporting Information

Dissection of Light-Induced Charge Accumulation at a Highly Active Iron Porphyrin: Insights in the Photocatalytic CO₂ Reduction

E. Pugliese, P. Gotico, I. Wehrung, B. Boitrel, A. Quaranta, M.-H. Ha-Thi, T. Pino, M. Sircoglou, W. Leibl, Z. Halime, A. Aukauloo**

Author Contributions

E.P. Formal analysis:Equal; Investigation:Equal; Writing – original draft:Supporting; Writing – review & editing:Supporting

P.G. Formal analysis:Supporting; Investigation:Supporting

I.W. Investigation:Supporting

B.B. Conceptualization:Supporting; Resources:Supporting

A.Q. Formal analysis:Equal; Investigation:Supporting

M.-H.H.-T. Formal analysis:Supporting; Funding acquisition:Equal; Investigation:Supporting

T.P. Formal analysis:Supporting; Investigation:Supporting

M.S. Formal analysis:Equal; Investigation:Equal

W.L. Formal analysis:Equal; Funding acquisition:Equal; Investigation:Equal; Writing – original draft:Supporting; Writing – review & editing:Supporting

Z.H. Conceptualization:Equal; Formal analysis:Equal; Funding acquisition:Equal; Investigation:Lead; Project administration:Equal; Supervision:Equal; Writing – original draft:Equal; Writing – review & editing:Equal

A.A. Conceptualization:Lead; Formal analysis:Equal; Supervision:Lead; Writing – original draft:Equal; Writing – review & editing:Equal

Supporting Information
©Wiley-VCH 2021
69451 Weinheim, Germany

Dissection of the Light Induced Charge Accumulation at Iron Porphyrin for a Highly Active Photocatalytic CO₂ Reduction

Eva Pugliese,^[a] Philipp Gotico,^[b] Iris Wehrung,^[a] Bernard Boitrel,^[c] Annamaria Quaranta,^[d] Minh-Huong Ha-Thi,^[b] Thomas Pino,^[b] Marie Sircoglou,^[a] Winfried Leibl,^[d] Zakaria Halime,^{*[a]} Ally Aukauloo,^{*[a,d]}

Abstract: Using light energy to drive multielectron catalytic reduction of CO₂ to produce a fuel is a contemporary research thrust. Recent efforts in the design of porphyrin-based catalysts have positioned them among the most performant electrocatalysts for CO₂ reduction. Powering these catalysts with the help of photosensitizers to realize light-driven catalysis comes along with a couple of unsolved challenges that need to be addressed with much vigor. We have designed an iron porphyrin catalyst decorated with urea functions (**UrFe**) acting as a multipoint hydrogen bonding scaffold towards the CO₂ substrate. When powered by a molecular photosensitizer in presence of an electron donor and water, a spectacular photocatalytic activity reaching unreported TONs and TOFs as high as 7270 and 3720 h⁻¹ respectively are observed. Importantly, we have spectroscopically characterized all the photo-reduced Fe^{II}, Fe^I and Fe⁰ states and compared with the electrochemically generated ones. While the Fe⁰ redox state has been widely accepted as the catalytically active species, we show here that the Fe^I species is already involved in the CO₂ activation which represents the rate determining step in the photocatalytic cycle. DFT calculations bring support to our experimental findings that constitute a new paradigm in the catalytic reduction of CO₂.

DOI: 10.1002/anie.2021XXXXX

Table of Contents

1. Experimental Procedures	4
Photocatalysis	4
Photoaccumulation.....	4
UV-vis spectroelectrochemistry	4
IR spectroelectrochemistry	4
2. Electrochemical data	5
Table S1	5
Figure S1.....	5
3. Photocatalysis	5
Table S2.....	5
Figure S2.....	6
Figure S3.....	6
Figure S4.....	7
Figure S5.....	7
Figure S6.....	7
Figure S7.....	8
Figure S8.....	8
Figure S9.....	8
Figure S10.....	9
Figure S11.....	9
Figure S12.....	9
4. UV-vis spectroscopy	10
Figure S13.....	10
Figure S14.....	10
Figure S15.....	11
Figure S16.....	11
Figure S17.....	12
Figure S18.....	12
Figure S19.....	12
Figure S20.....	13
5. Infrared spectroscopy	13
Figure S21	13
Figure S22.....	14
6. Computational study	14
Figure S23.....	15

SUPPORTING INFORMATION

Figure S24.....	15
Table S3.....	16
Figure S25.....	16
Figure S26.....	17
Figure S27.....	17
Table S4.....	18
Table S5.....	21
References.....	24

SUPPORTING INFORMATION

1. Experimental Procedures

General Materials

The syntheses of **UrFe**, **F₂₀TPPFe** and **TPPFe** were previously reported by our group.^[1] 1,3-dimethyl-2-phenyl-2,3-dihydro-1*H*-benzo[d]imidazole (BIH) was prepared as found in the literature.^[2] Solvents, photosensitizers and electrolyte salts were purchased from Sigma Aldrich or Carlo Erba (N,N-dimethylformamide).

Photocatalysis

Photocatalysis experiments were performed in 41.5 mL glass vials hermetically closed with a septum and containing 6.5 mL of solution and an 8 mm stir bar. The reaction mixture was first purged with CO₂ during 30 min, while kept in the dark, and then irradiated with LED light source (SugarCube).

The gas phase was automatically injected and analyzed by a Micro GC Fusion Gas Analyser (Inficon). In module A (PLOT column with molecular sieve and 10 m length) a 9 s backflush is applied to separate H₂, O₂, N₂, CH₄ and CO. Module B (RT-Q-bond column of 12 m) allows the detection of heavier molecules, such as CO₂, H₂O vapor and C₂ products. The setup is equipped of an Ar carrier gas with 99.999% purity and a TCD detector.

For experiments with limited amount of CO₂, the reaction vial was first degassed with Ar, then different amounts of a solution of 10 mL of DMF previously purged for 20 min with CO₂ were injected. The solubility of CO₂ in DMF was taken to be 230 mM[ref].

To quantify products, calibration was manually performed injecting fixed aliquots (100 or 500 μL) of reference gasses in the same vial used in a typical run, filled with 6.5 mL of the same solvent mixture and an 8 mm stirring bar, and purged for 30 min with CO₂. Calibration curves were fitted with 10 points choosing the same range of area peaks obtained experimentally.

Turnover numbers (TON) were calculated from chromatograms quantification as the number of moles of product over the number of moles of catalyst.

Turnover frequencies (TOF) were calculated from the slope of the TON evolution over time, considering the initial linear region, but cutting out the point zero linked to artefacts of catalysis activation (small inflection due to bubble formation).

Labeled ¹³CO₂ photocatalysis was done as described above, but purging with a ¹³CO₂ bottle of Sigma Aldrich. ¹³CO was detected by manual sampling (50 μL) from the headspace of the reaction cells into a TraceGC Ultra / ISQ GC/MS system (Thermo Scientific) equipped with a TraceGOLD TG-5MS 30 m, 0.25 mm diameter column (Thermo Scientific) kept at 313 K using helium carrier gas.

Photoaccumulation

Photoaccumulation experiments were conducted in a 1 cm optical path quartz cuvette hermetically closed with a septum. To probe the sample a Agilent Technologies Cary 60 UV-Vis spectrophotometer was used, adapted with a liquid nitrogen dewar and thermostated around the cuvette to perform measurements down to -196°C. This apparatus is connected to the temperature controller (CoolSpek UV USP-203 by Unisoku), able to regulate the flux of liquid nitrogen and to heat the cuvette. During the measurement, the sample is irradiated with a blue LED light source (SugarCube). The solution is stirred during the measurement. Spectra acquisition is operated through the CaryWin software, in the Scanning Kinetics mode.

UV-vis spectroelectrochemistry

UV-vis spectroelectrochemical measurements were done in a quartz cuvette with Pt honeycomb electrode (PINE research) and a Pt wire pseudo-reference electrode. To probe the sample the spectrophotometer Agilent Technologies Cary 50 UV-Vis was used. The potentials were applied through the potentiostat Metrohm Autolab 204 in the chronoamperometry method.

IR-spectroelectrochemistry

Infrared spectroelectrochemical measurements were recorded with an FT-IR Thermo Scientific Nicolet 6700 spectrometer, with ATR diamond accessory. A home-made PTFE electrochemical cell fitted ATR crystal was filled with 1 mL of THF solution containing 1 mM catalyst and 0.1 M TBAPF₆ in a three-electrode system including a GC working electrode, Pt counter electrode and Ag/AgNO₃ (10 mM) reference electrode (+0.54 V vs. NHE) under a continuous flow of Argon or CO₂. Applied potential was varied by 200 mV steps and three infrared spectra were recorded for each potential applied.

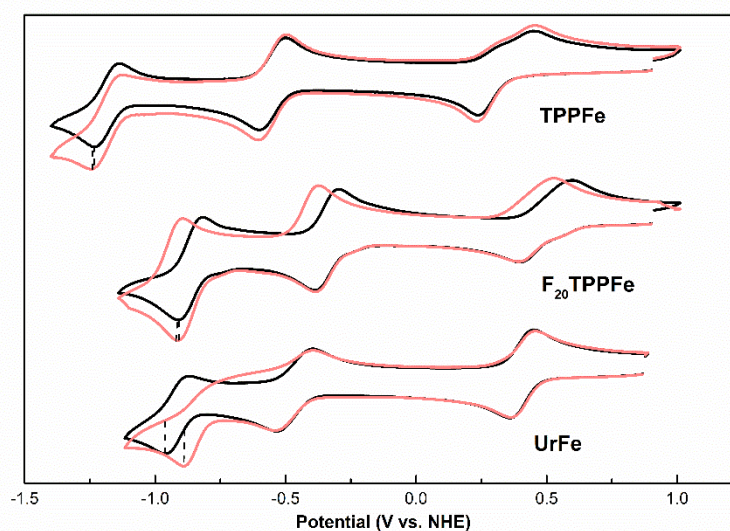
SUPPORTING INFORMATION

2. Electrochemical data

Table S1 Electrochemical potentials in Volts of the studied compounds vs NHE in 0.1 M TBAPF₆ Ar-saturated DMF_{dry} solution.

Entry	Compound	E ^{1/2} (M/M ⁻)	E ^{1/2} (M ⁻ /M ²⁻)	E ^{1/2} (M ²⁻ /M ³⁻)	Ref.
1	UrFe	0.23	-0.63	-1.12	[1]
2	TPPFe	0.09	-0.79	-1.42	[1]
3	F ₂₀ TPPFe	0.25	-0.59	-1.11	[1]
4	Ru(bpy) ₃ ²⁺ [a]	-1.09			[3]
5	Ir(ppy) ₃ ⁺ [a]	-1.95			[3]

[a] In acetonitrile solution.

**Figure S1.** Cyclic voltammograms of the studied iron porphyrins in Ar (black) and CO₂ (red) atmospheres, 1 mM catalyst, 0.1 M TBAPF₆ in DMF_{dry}, 100 mV s⁻¹.

3. Photocatalysis

Table S2 Photocatalysis experiments performed with 20 μM catalyst, 1 mM Ru(bpy)₃²⁺, BIH as SED in DMF/H₂O 9:1 under LED irradiation (100 W m⁻²) for 2h.

	Catalyst	[SED] (mM)	LED type	CO (μmol)	H ₂ (μmol)	Selectivity (CO %)	TON _{CO}	TOF _{CO} (h ⁻¹)
1	UrFe ^[a]	50	Blue	8	0.7	92	63	46
2	UrFe ^[b]	100	Blue	2.7	0.6	82	21	14.6
3	-	50	Blue	50	0.4	99	-	-
4	UrFe ^[c]	50	White	0	-	-	0	-
5	UrFe ^[d]	50	White	0.9	0	100	7	3.5
6	UrFe ^[e]	50	Blue	65	0.1	100	623	497

[a] In ACN/H₂O 9:1 solvent mixture. [b] Sodium ascorbate used as SED in ACN/H₂O 6:4. [c] No photosensitizer in the reaction mixture. [d] Ir(ppy)₃ is used as photosensitizer and TEA as electron donor. [e] No water in the solvent mixture.

SUPPORTING INFORMATION

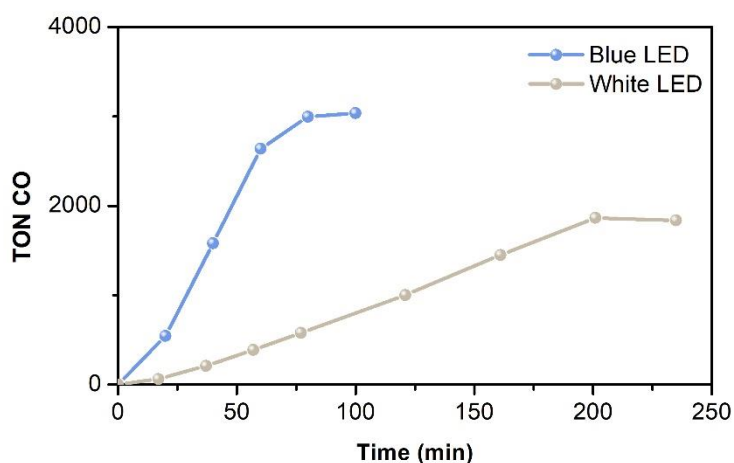


Figure S2 Time evolution of CO produced under light irradiation with a blue LED (blue dots, $\lambda_{em}=460$ nm 100 W m^{-2}) and white LED (grey dots, $\lambda > 405$ nm 100 W m^{-2}) of **UrFe** as catalyst with 20 μ M concentration; $[Ru(bpy)_3]^{2+}$ photosensitizer 1 mM, BIH sacrificial electron donor 50 mM in CO_2 -saturated DMF/ H_2O 9:1

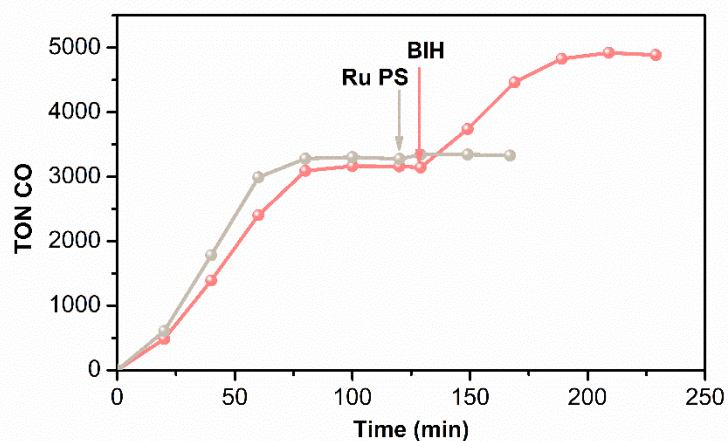


Figure S3 Time evolution of CO produced under light irradiation with a blue LED ($\lambda_{em}=460$ nm 100 W m^{-2}) of **TPPFe-Ur** as catalyst with 20 μ M concentration; $[Ru(bpy)_3]^{2+}$ photosensitizer 1 mM, BIH sacrificial electron donor 50 mM in CO_2 -saturated DMF/ H_2O 9:1. The arrows indicate the point of reinjection of 1 mL of 2 mM $[Ru(bpy)_3]^{2+}$ (beige) or 1 mL of 0.2 M BIH (red).

SUPPORTING INFORMATION

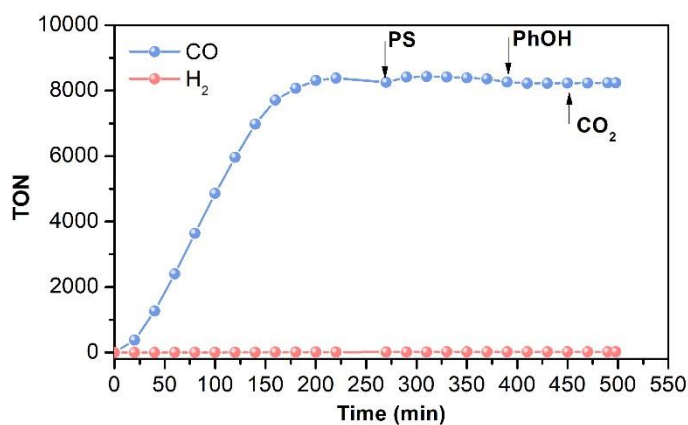


Figure S4 Time evolution of CO (blue) and H₂ (red) produced under light irradiation with a blue LED ($\lambda_{em}=460$ nm 100 W m⁻²) of **UrFe** as catalyst with 20 μ M concentration; [Ru(bpy)₃]²⁺ photosensitizer 1 mM, BIH sacrificial electron donor 250 mM in CO₂-saturated DMF/H₂O 9:1. The arrows indicate the re-injections of the photosensitizer (PS), of a proton source (PhOH) and rebubbling of CO₂.

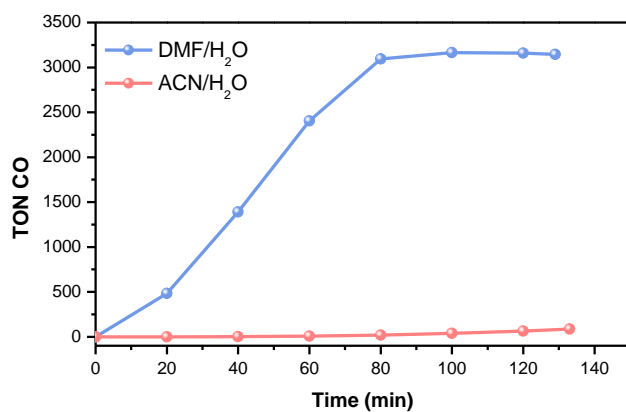


Figure S5 Time evolution of CO produced under light irradiation with a blue LED ($\lambda_{em}=460$ nm 100 W m⁻²) of **UrFe** as catalyst with 20 μ M concentration; [Ru(bpy)₃]²⁺ photosensitizer 1 mM, BIH sacrificial electron donor 50 mM in CO₂-saturated DMF/H₂O 9:1 (blue) and CO₂-saturated ACN/H₂O 9:1 (red).

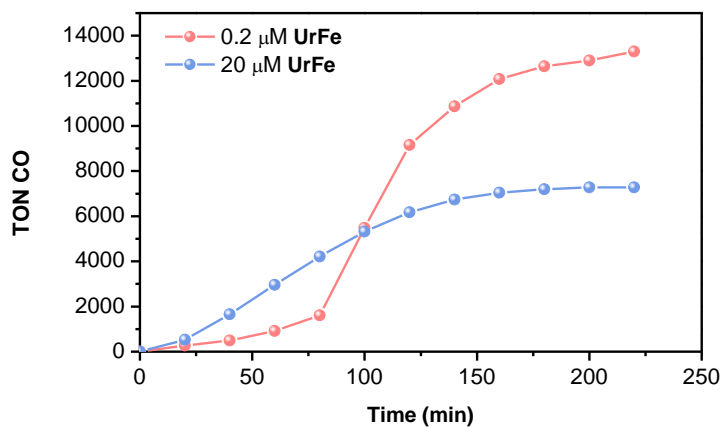


Figure S6. Time evolution of CO produced under light irradiation with a blue LED ($\lambda_{em}=460$ nm 100 W m⁻²) of **UrFe** as catalyst with 20 μ M concentration (blue) and 0.2 μ M concentration (red); [Ru(bpy)₃]²⁺ photosensitizer 1 mM, BIH sacrificial electron donor 250 mM in CO₂-saturated DMF/H₂O 9:1.

SUPPORTING INFORMATION

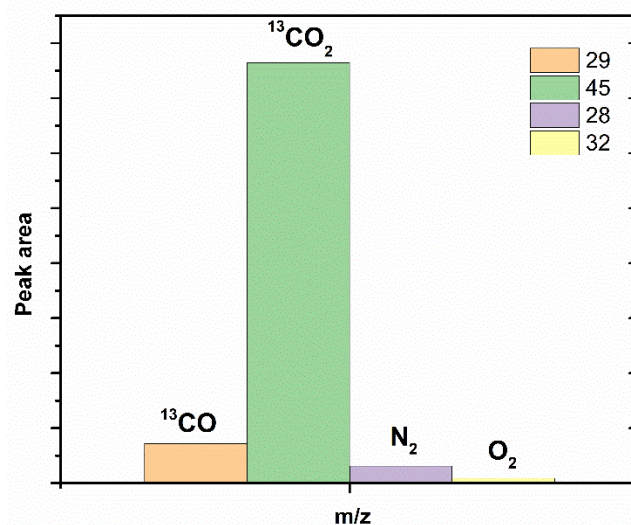


Figure S7 GC/MS analysis of 50 μL of gas mixture produced upon 1 h irradiation with blue LED ($\lambda_{\text{em}}=460\text{ nm}$ 100 W m^{-2}) of 20 μM **UrFe** catalyst; 1 mM $[\text{Ru}(\text{bpy})_3]^{2+}$ photosensitizer, 50 mM BIH sacrificial electron donor $^{13}\text{CO}_2$ -saturated DMF/ H_2O 9:1.

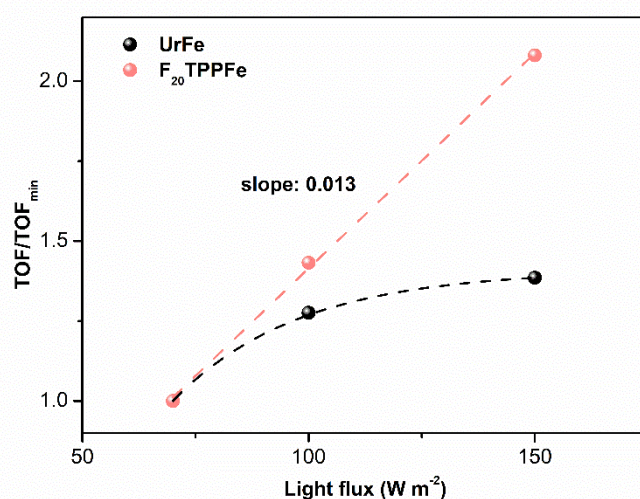


Figure S8 Dependency of the reaction kinetics (TOF) on the light flow for **UrFe** (red) and for **F₂₀TPPFe** (black). 20 μM catalyst, 1 mM $[\text{Ru}(\text{bpy})_3]^{2+}$ photosensitizer, 50 mM BIH sacrificial electron donor in CO_2 -saturated DMF/ H_2O 9:1, blue LED irradiation ($\lambda_{\text{em}}=460\text{ nm}$).

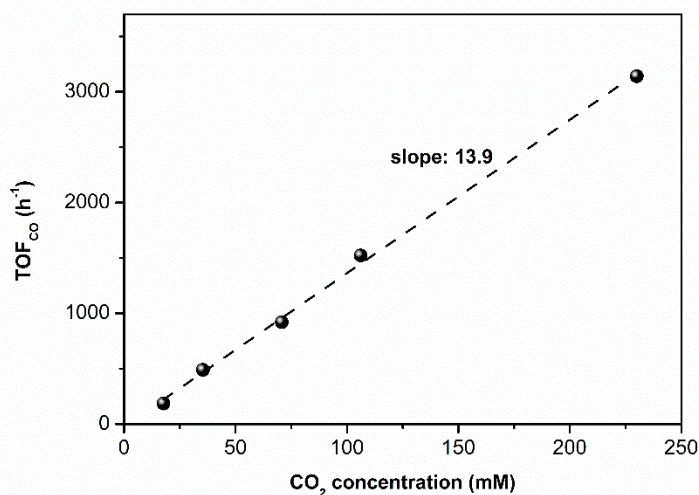


Figure S9 Dependency of the reaction kinetics (TOF) on the amount of CO_2 added for **UrFe** 20 μM catalyst, 1 mM $[\text{Ru}(\text{bpy})_3]^{2+}$ photosensitizer, 50 mM BIH sacrificial electron donor in DMF/ H_2O 9:1, blue LED irradiation ($\lambda_{\text{em}}=460\text{ nm}$ 100 W m^{-2}).

SUPPORTING INFORMATION

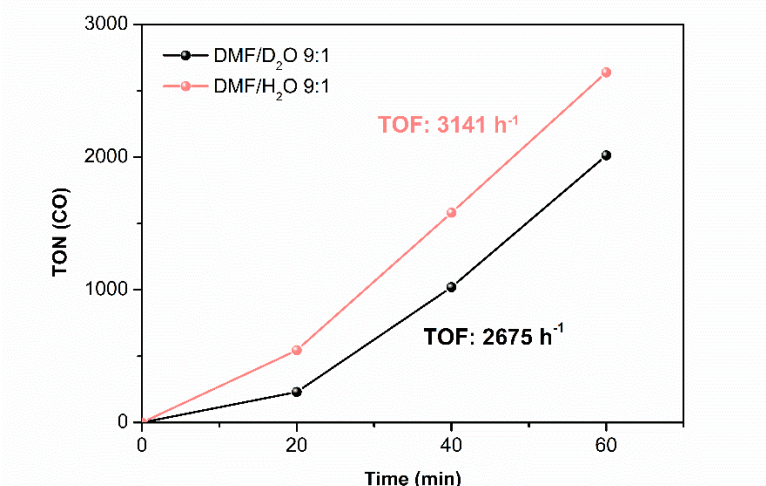


Figure S10 Time evolution of CO produced under light irradiation with a blue LED ($\lambda_{em}=460$ nm 100 W m^{-2}) of **UrFe** as catalyst with 20 μ M concentration; $[Ru(bpy)_3]^{2+}$ photosensitizer 1 mM, BIH sacrificial electron donor 50 mM in CO_2 -saturated DMF/ H_2O 9:1 (red) and CO_2 -saturated DMF/ D_2O 9:1 (black).

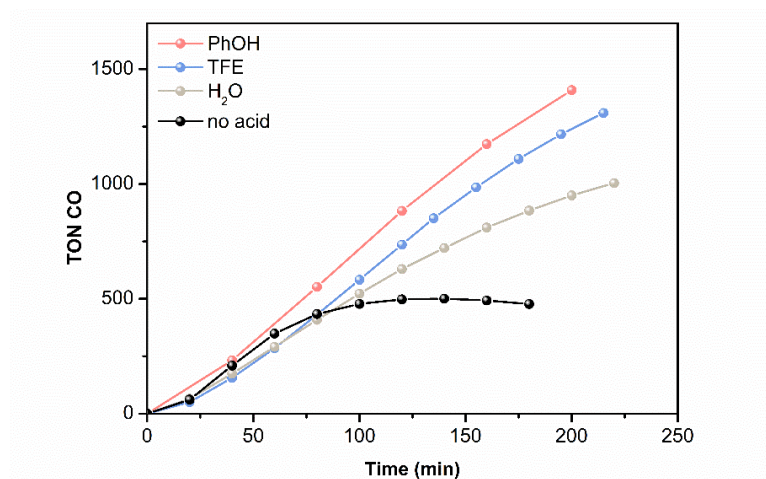


Figure S11. Time evolution of CO produced under light irradiation with a white LED ($\lambda > 405$ nm, 100 W m^{-2}) of **UrFe** as catalyst with 20 μ M concentration; $[Ru(bpy)_3]^{2+}$ photosensitizer 1 mM, BIH sacrificial electron donor 50 mM in CO_2 -saturated DMF and 100 mM PhOH (red), 100 mM TFE (blue), 100 mM H_2O (grey) or in absence of proton (black).

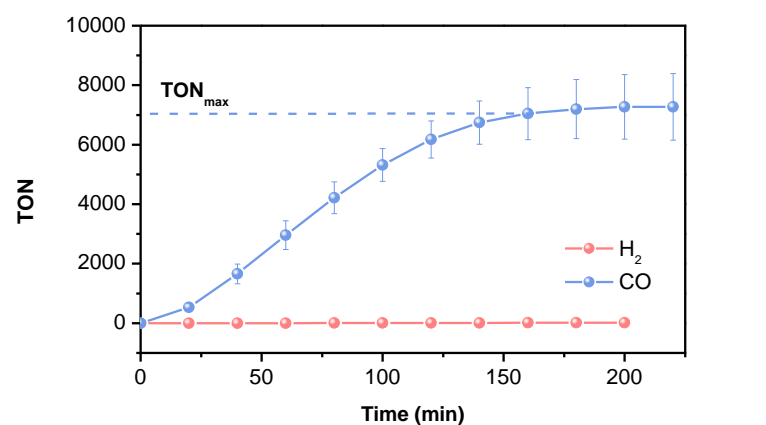


Figure S12 Time evolution of CO (blue) and H_2 (red) produced under light irradiation with a blue LED ($\lambda_{em}=460$ nm 100 W m^{-2}) of **UrFe** as catalyst with 20 μ M concentration; $[Ru(bpy)_3]^{2+}$ photosensitizer 1 mM, BIH sacrificial electron donor 250 mM in CO_2 -saturated DMF/ H_2O 9:1. The data is the average of 3 runs, error bars represent the standard error.

SUPPORTING INFORMATION

4. UV-vis spectroscopy

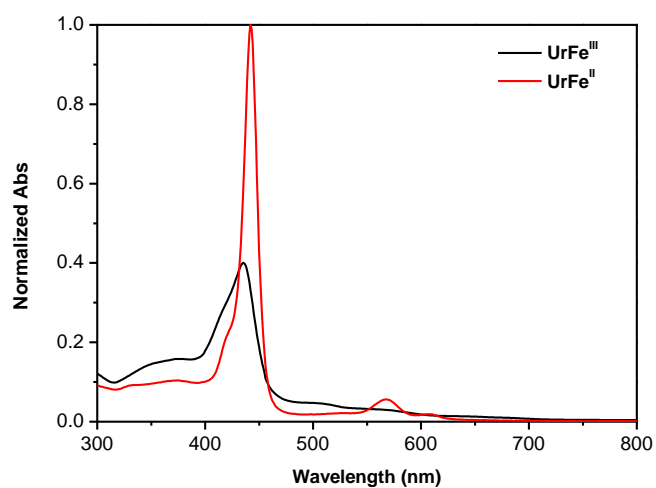


Figure S13 UV-vis reference spectra of UrFe^{III} (black) in Ar-saturated DMF, and chemically prepared UrFe^{II} (red) with ZnHg amalgam in N_2 -saturated DMF.

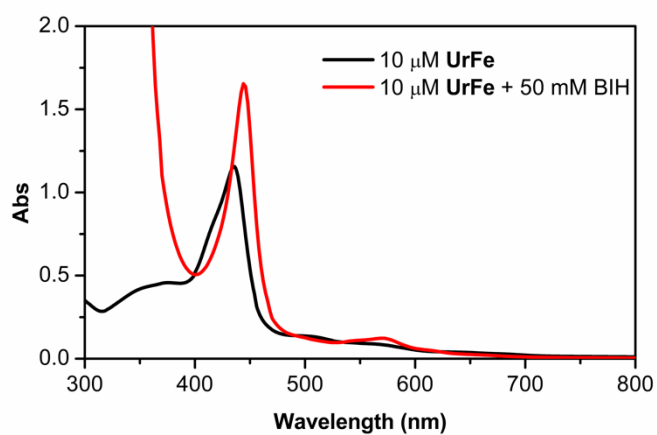


Figure S14 UV-vis reference spectra of UrFe in Ar-saturated DMF before (black) and after the addition of 50 mM of BIH (red).

SUPPORTING INFORMATION

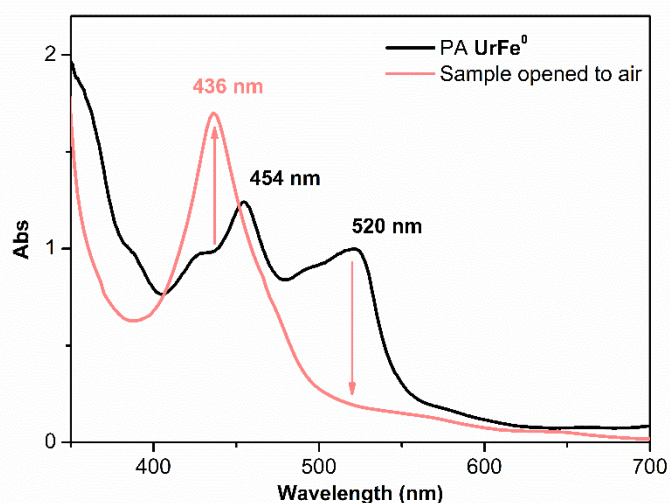


Figure S15 UV-vis spectra of photoaccumulated (blue LED irradiation) UrFe 10 μM , $[\text{Ru}(\text{bpy})_3]^{2+}$ 30 μM , BIH 7 mM in N_2 -saturated DMF_{dry} at -35°C before (black) and after (red) opening the sample to the air.

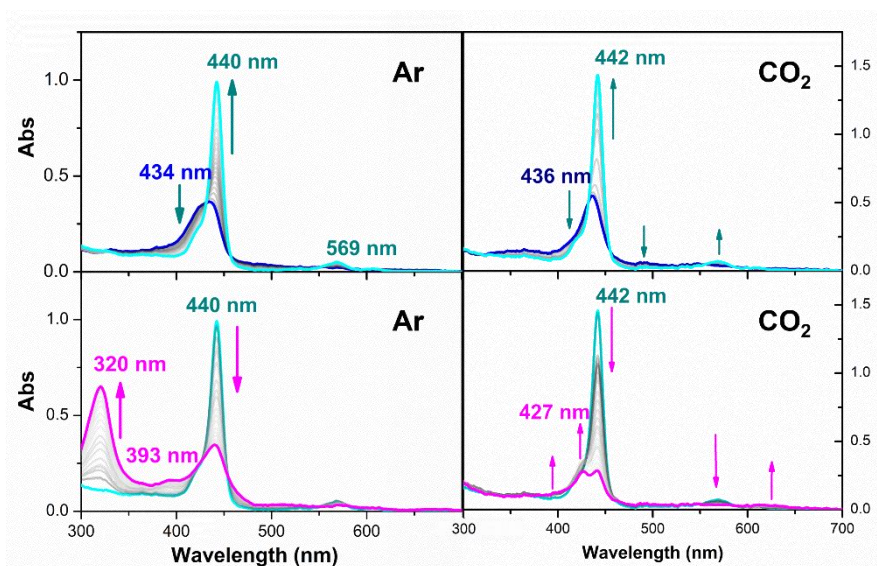


Figure S16 UV-vis spectral evolution in spectroelectrochemistry experiment with UrFe 40 μM in Ar-saturated DMF_{dry} (left) and CO_2 -saturated DMF_{dry} (right), 0.2 M TBAPF_6 , Pt Working Electrode, Pt Counter Electrode and Ag pseudo-Reference Electrode; Room Temperature. Top: Fe^{III} to Fe^{II} reduction; Bottom: Fe^{II} to Fe^{I} reduction

SUPPORTING INFORMATION

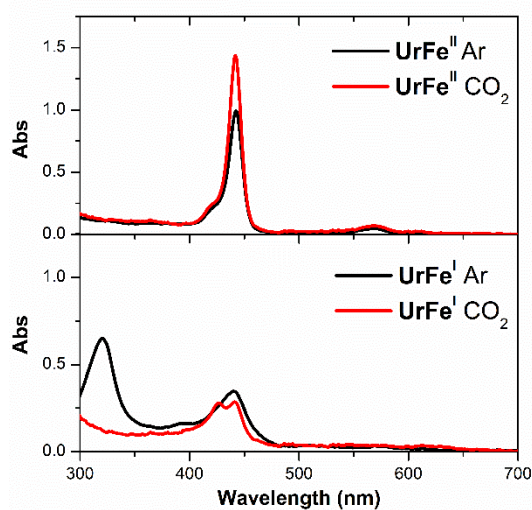


Figure S17 UV-vis spectra obtained in spectroelectrochemistry experiment with UrFe 40 μM in 0.2 M TBAPF_6 DMF_{dry} solution in Ar (black) and CO_2 (red) atmosphere. Top: UrFe^{II} , bottom: UrFe^{I} . Pt Working Electrode, Pt Counter Electrode and Ag pseudo-Reference Electrode; Room Temperature. (See Figure S17)

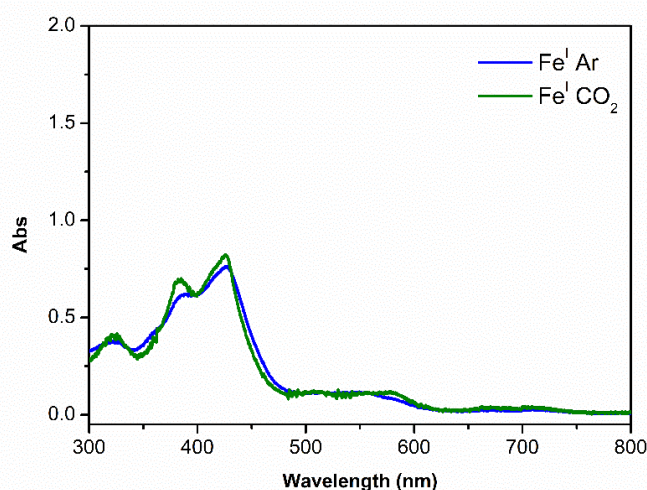


Figure S18 UV-vis spectral evolution in spectroelectrochemistry experiment with $\text{F}_{20}\text{TPPFe}$ 40 μM in DMF_{dry} , 0.2 M TBAPF_6 , Pt Working Electrode, Pt Counter Electrode and Pt pseudo-Reference Electrode; Room Temperature.

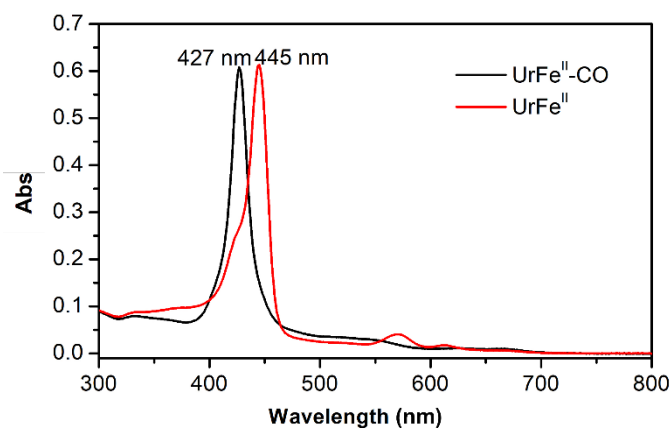


Figure S19 UV-vis reference spectra of chemically prepared UrFe^{II} in N_2 -saturated DMF (red) and with CO -saturated DMF (black).

SUPPORTING INFORMATION

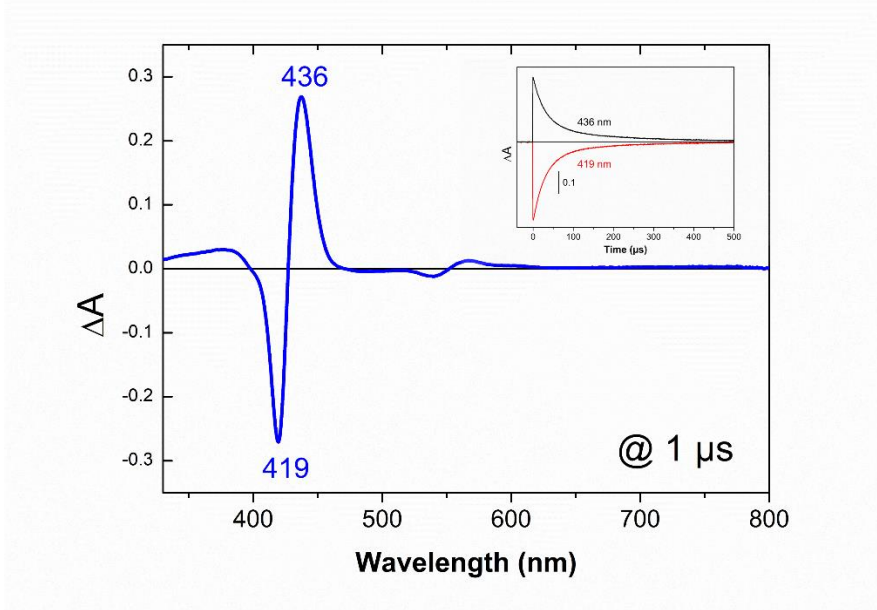


Figure S20 UV-vis laser flash photolysis of UrFe (OD 420=1), in CO-saturated ACN/H₂O 9/1, 25 mM NaAsc, exc 460 nm, 15 mJ

5. Infrared spectroscopy

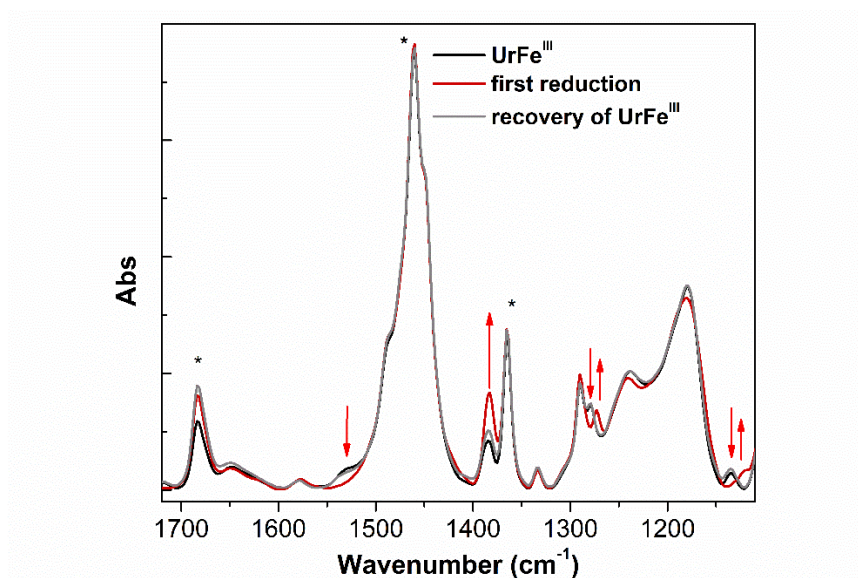


Figure S21 IR reversible conversion of Fe^{III} to Fe^{II} in spectroelectrochemistry experiment with UrFe 1 mM in Ar-saturated THF, 0.1 M TBAPF₆, GC Working Electrode, Pt Counter Electrode and AgNO₃/Ag Reference Electrode; Room Temperature. Peaks with asterisk are due to the solvent.

SUPPORTING INFORMATION

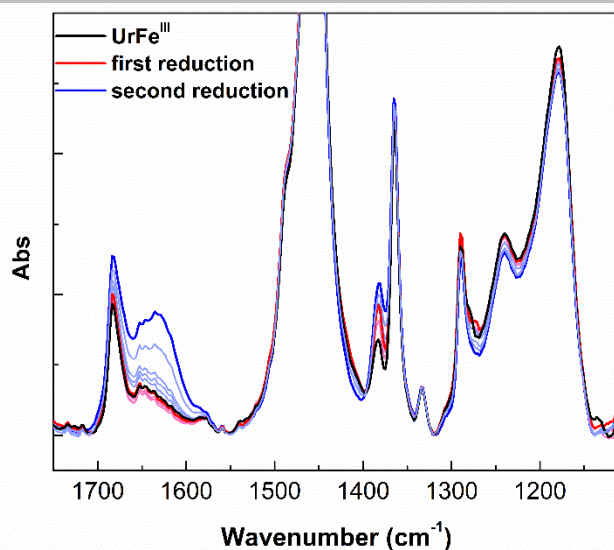
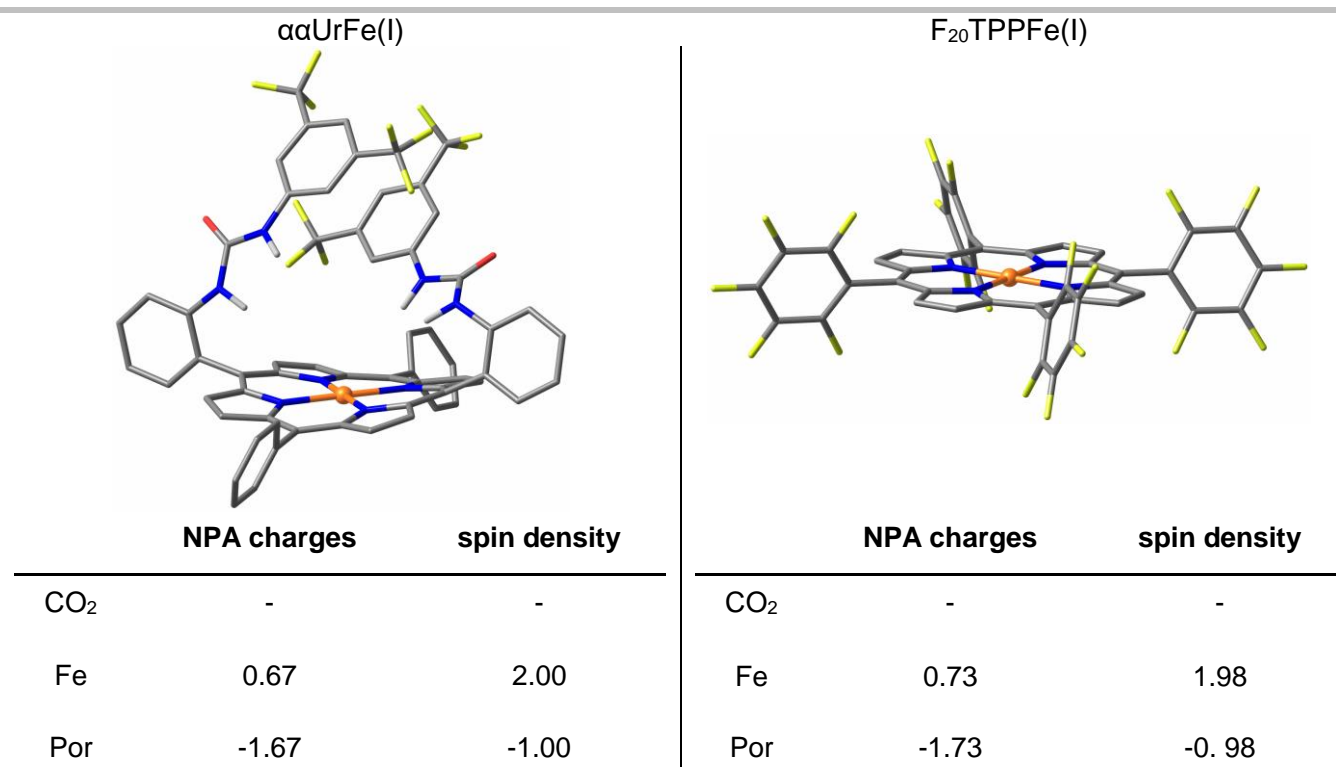
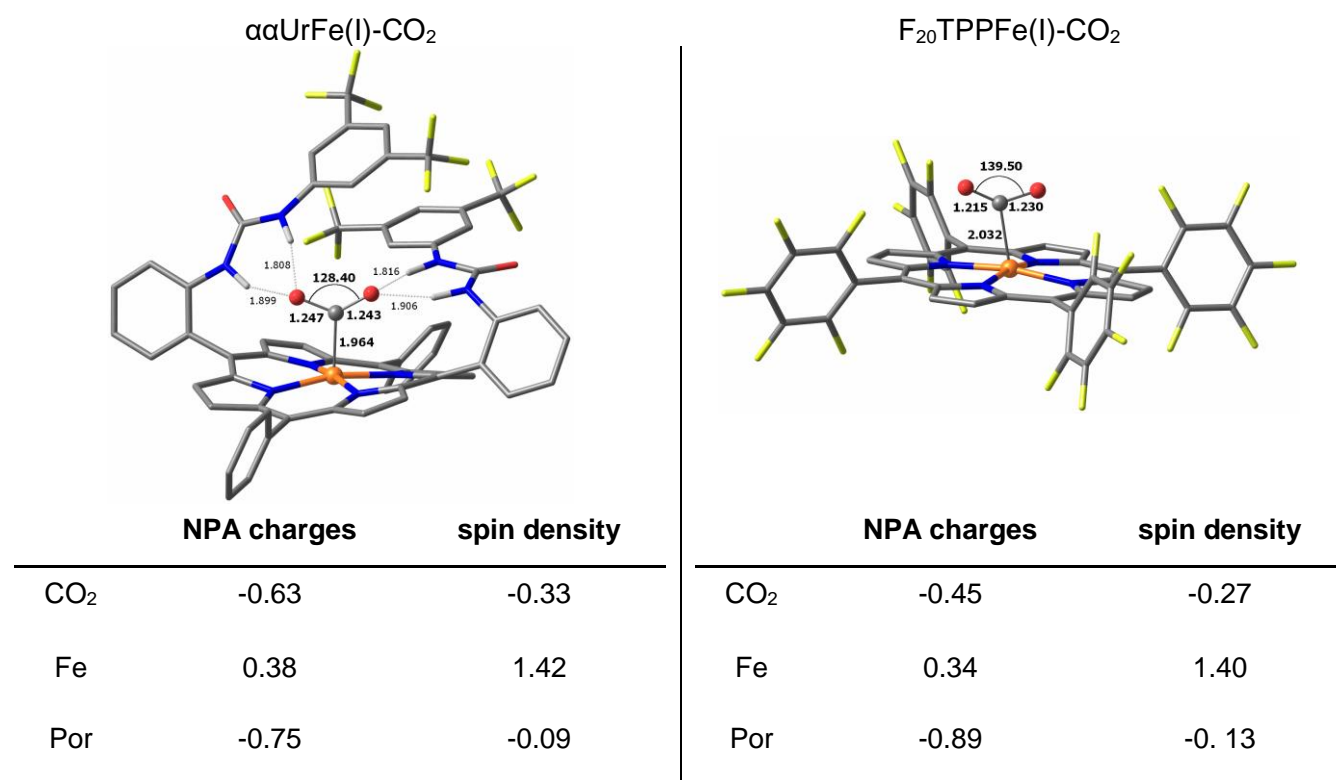


Figure S22 IR spectral evolution in spectroelectrochemistry experiment with **UrFe** 1 mM in CO₂-saturated THF. Black: **UrFe^{III}**, Red: **UrFe^{II}**, Blue: **UrFe^I**

6. Computational study

DFT calculations were performed using the Gaussian 16 program package.^[4] PBE0^[5] functional was used to predict geometries and relative energies.^[6,7] B3LYP^[8] was used for the calculation of vibrational spectra. In both cases, dispersion correction with Becke-Johnson damping (D3BJ)^[9] was introduced to better reproduce the weak interactions occurring at the 2nd sphere coordination and solvent effects (DMF) were included using the CPCM approach.^[10] Lan1d2z with ECP^[11] and 6-31G(d)^[12] basis sets were chosen for Fe and main group atoms respectively. To speed up the calculations, the two arms at the opposite of the coordination face of the porphyrin were replaced with protons. The corresponding model porphyrin is denoted **ααUr**. The F₂₀TPPF_e was optimized as is. The geometry of intermediates were optimized as singlet, open singlet (S=1) and triplet (S=3) for formally Fe(II) species, and as doublet (S=2) for Fe(I) species. Only the most stable configurations are detailed herein. IR spectra were generated by convoluting the theoretical stick spectra with a Gaussian fit (half-width $W_{1/2} = 15 \text{ cm}^{-1}$). Figures, charges and spin analysis were performed using ChemCraft program.^[13]

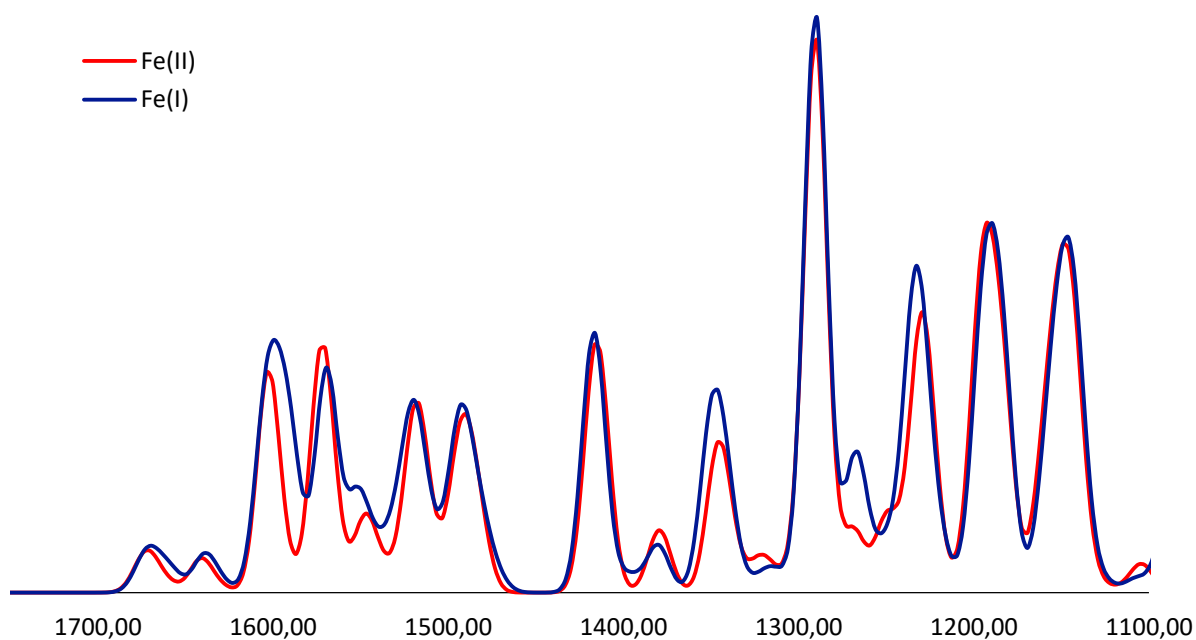
SUPPORTING INFORMATION

Figure S23 PBE0 geometries, partial charges and spin densities of α UrFe^I and F₂₀TPPFe^IFigure S24 PBE0 geometries, partial charges and spin densities of α UrFe^I-CO₂ and F₂₀TPPFe^I-CO₂

SUPPORTING INFORMATION

Table S3 Predicted CO₂ binding energies, dissociation and association constant, and expected half-wave potential change^[4] in the Fe(I) oxidation state at 298K

	ΔG_{coord} (kcal/mol)	k_D (M ⁻¹)	k_A (M ⁻¹)	ΔE (V)
$\alpha\alpha\text{UrFe(I)}$	0.78	0.87	1.16	0.006
$\text{F}_{20}\text{TPPFe(I)}$	10.46	$1.09 \cdot 10^7$	$9.19 \cdot 10^8$	0.000

**Figure S25** Theoretical IR band spectra (gaussian fit $w_{1/2}=15 \text{ cm}^{-1}$) obtained for Red: $\alpha\alpha\text{UrFe}^{\text{II}}$, Blue: $\alpha\alpha\text{UrFe}^{\text{I}}$

SUPPORTING INFORMATION

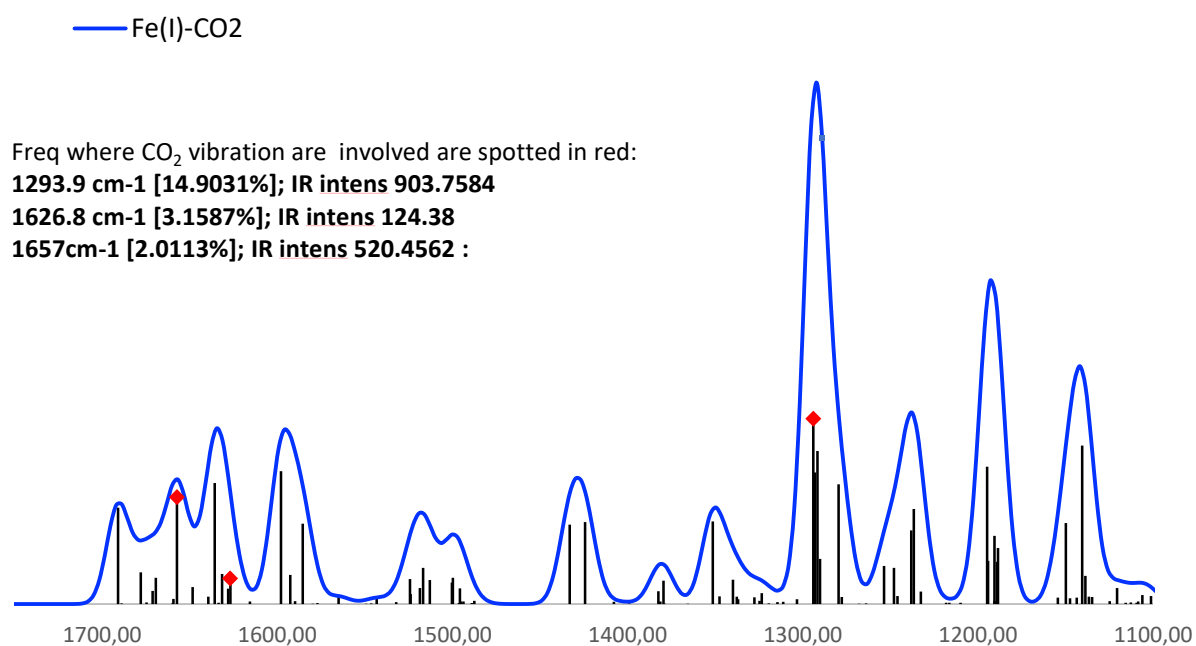


Figure S26 Theoretical IR stick and band spectrum (gaussian fit $w_{1/2}=15\text{ cm}^{-1}$) obtained for $\alpha\alpha\text{UrFe}^{\text{I}}\text{-CO}_2$

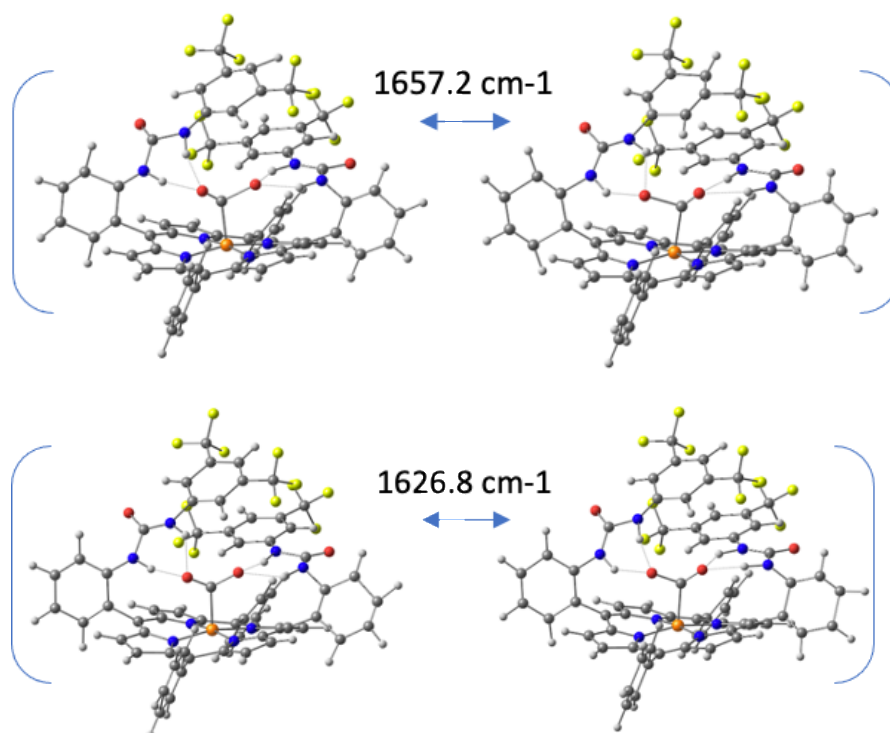


Figure S27 Vibration modes associated with the CO₂ fragment in $\alpha\alpha\text{UrFe}^{\text{I}}\text{-CO}_2$

SUPPORTING INFORMATION

Table S4 xyz coordinates (charge, spin multiplicity) and energetics (E (G) at 298K) at the PBE0 level

$\alpha\text{UrFe}^{\text{II}} (0,3)$				$\alpha\text{UrFe}^{\text{I}} (-1,2)$			
-4290.147976 (-4289.390599) Hartrees				-4290.27915891 (-4477.90691) Hartrees			
C	0.699866000000	0.663492000000	3.108864000000	C	1.519161000000	4.679451000000	0.962039000000
C	0.498759000000	-0.660109000000	3.499933000000	C	1.975510000000	5.714954000000	1.775729000000
C	1.076032000000	-1.739592000000	2.828643000000	H	2.728689000000	5.493660000000	2.526912000000
C	0.701163000000	-3.109721000000	3.046463000000	C	1.469301000000	7.004918000000	1.641612000000
H	0.002137000000	-3.450056000000	3.796915000000	H	1.828119000000	7.801237000000	2.286513000000
C	1.362739000000	-3.851001000000	2.117761000000	C	0.500481000000	7.260467000000	0.674277000000
H	1.324981000000	-4.920627000000	1.963808000000	H	0.099295000000	8.263248000000	0.557403000000
C	2.171719000000	-2.937730000000	1.359710000000	C	0.041333000000	6.247172000000	-0.161254000000
C	3.027647000000	-3.335044000000	0.329672000000	H	-0.707703000000	6.448557000000	-0.915929000000
C	3.950400000000	-2.482108000000	-0.270605000000	C	0.545259000000	4.951689000000	-0.020306000000
C	4.986833000000	-0.707358000000	-1.165232000000	C	-1.095400000000	3.708353000000	-1.393061000000
H	5.130741000000	-3.941040000000	-1.494186000000	C	-2.363129000000	1.814123000000	-2.374485000000
C	5.743913000000	-1.829230000000	-1.450205000000	C	-2.231949000000	0.500623000000	-2.844445000000
H	6.630126000000	-1.776666000000	-2.066212000000	H	-1.244857000000	0.063983000000	-2.963885000000
C	5.117029000000	-0.800457000000	-0.800457000000	C	-3.357898000000	-0.260089000000	-3.119489000000
C	5.491839000000	0.622885000000	-0.997549000000	C	-4.636936000000	0.257886000000	-2.938248000000
C	4.726503000000	1.695618000000	-0.536895000000	H	-5.513720000000	-0.349347000000	-3.124817000000
C	4.941758000000	3.060430000000	-0.943245000000	C	-4.755499000000	1.563493000000	-2.481246000000
H	5.754254000000	3.399459000000	-1.570038000000	C	-3.642703000000	2.352842000000	-2.210070000000
C	3.922726000000	3.791111000000	-0.421617000000	H	-3.753682000000	3.365273000000	-1.849126000000
H	3.738234000000	4.852138000000	-0.519636000000	N	1.525706000000	1.075808000000	2.086634000000
C	3.110092000000	2.881974000000	0.342508000000	N	1.984027000000	-1.653044000000	1.798932000000
C	2.015796000000	3.281398000000	1.107758000000	N	4.041410000000	-1.129227000000	-0.057339000000
C	1.335431000000	2.428978000000	1.979402000000	N	3.606392000000	1.605807000000	0.253190000000
C	0.374804000000	2.879861000000	2.948237000000	N	0.851778000000	-3.672285000000	-1.281394000000
H	0.048406000000	3.903896000000	3.064363000000	H	1.416002000000	-2.833184000000	-1.333849000000
C	0.008577000000	1.790890000000	3.673754000000	N	-0.658337000000	-2.182792000000	-0.411444000000
H	-0.685206000000	1.743853000000	4.500545000000	H	0.142618000000	-1.574431000000	-0.302909000000
C	-0.420225000000	-0.958217000000	4.629828000000	N	0.153358000000	3.890922000000	-0.849037000000
C	-1.789352000000	-0.684089000000	4.541842000000	H	0.735362000000	3.068029000000	-0.756035000000
H	-2.187379000000	-0.234100000000	3.638879000000	N	-1.193602000000	2.496037000000	-2.053298000000
C	-2.639112000000	-0.987485000000	5.601969000000	H	-0.347064000000	1.952024000000	-2.149367000000
H	-3.700656000000	-0.771981000000	5.517690000000	O	-1.211991000000	-4.410994000000	-0.606205000000
C	-2.132753000000	-1.570682000000	6.761812000000	O	-2.006968000000	4.518745000000	-1.317944000000
H	-2.796894000000	-1.807604000000	7.588211000000	Fe	2.786596000000	-0.023783000000	1.017923000000
C	-0.770819000000	-1.850693000000	6.856505000000	H	1.141829000000	-1.765964000000	5.869353000000
H	-0.368025000000	-2.304235000000	7.757792000000	H	7.770367000000	1.792002000000	-0.161101000000
C	0.079496000000	-1.548652000000	5.796541000000	C	-3.063085000000	1.716761000000	1.300281000000
C	2.785943000000	-4.687690000000	-0.242089000000	F	-4.107449000000	2.436852000000	0.863503000000
C	3.594616000000	-5.799450000000	-0.015358000000	F	-3.138812000000	1.711720000000	2.646341000000
H	4.493966000000	-5.687621000000	0.583757000000	F	-1.945125000000	2.385162000000	0.976912000000
C	3.232480000000	-7.047444000000	-0.519780000000	C	-5.600817000000	-2.285858000000	-0.189174000000
H	3.862959000000	-7.910748000000	-0.329063000000	F	-5.475903000000	-3.453930000000	-0.831555000000
C	2.057279000000	-7.187435000000	-1.254494000000	F	-6.238405000000	-2.532485000000	0.969408000000
H	1.769952000000	-8.161065000000	-1.640643000000	F	-6.425174000000	-1.510076000000	-0.919702000000
C	1.252206000000	-6.080829000000	-1.515980000000	C	-6.115322000000	2.110846000000	-2.166483000000
H	0.346166000000	-6.172027000000	-2.104615000000	F	-6.446168000000	1.890473000000	-0.877676000000
C	1.618949000000	-4.834750000000	-1.018724000000	F	-6.183189000000	3.437121000000	-2.359695000000
C	-0.411574000000	-3.499871000000	-0.748087000000	F	-7.073352000000	1.542286000000	-2.914452000000
C	-1.877537000000	-1.620773000000	-0.049795000000	C	-3.198566000000	-1.654564000000	-3.648613000000
C	-3.099216000000	-2.276829000000	-0.240163000000	F	-3.223638000000	-1.680836000000	-4.992602000000
H	-3.111098000000	-3.282206000000	-0.634604000000	F	-2.034664000000	-2.209846000000	-3.269584000000
C	-4.282206000000	-1.609825000000	0.044247000000	F	-4.185842000000	-2.461868000000	-3.225687000000
C	-4.289788000000	-0.306423000000	0.529416000000				
H	-5.222209000000	0.216211000000	0.706411000000				
C	-3.070134000000	0.325385000000	0.739920000000				
C	-1.869275000000	-0.318947000000	0.463949000000				
H	-0.926277000000	0.200088000000	0.614957000000				
C	6.698719000000	0.924468000000	-1.812205000000				
C	6.747334000000	0.615499000000	-3.176488000000				
H	5.887079000000	0.147978000000	-3.647917000000				
C	7.879894000000	0.914204000000	-3.928920000000				
H	7.901812000000	0.671970000000	-4.987733000000				
C	8.977374000000	1.528302000000	-3.328426000000				
H	9.860737000000	1.761455000000	-3.916138000000				
C	8.935780000000	1.845257000000	-1.972110000000				
H	9.787363000000	2.324223000000	-1.497099000000				
C	7.803238000000	1.546866000000	-1.219375000000				

SUPPORTING INFORMATION

C	2.364602000000	-0.025690000000	0.149549000000	C	3.287596000000	-2.281878000000	0.753182000000
H	1.394387000000	-0.480549000000	-0.007045000000	F	4.239169000000	-2.991240000000	0.097331000000
H	0.572771000000	1.517242000000	-0.657284000000	F	3.417091000000	-2.603719000000	2.064746000000
N	-0.995399000000	-3.749445000000	-1.245584000000	F	2.089960000000	-2.746295000000	0.343981000000
C	0.234040000000	-3.612369000000	-1.857790000000	C	6.149201000000	1.785005000000	0.957009000000
H	-1.484672000000	-2.875550000000	-1.049279000000	F	6.388079000000	2.889718000000	0.217695000000
N	0.389585000000	-2.321931000000	-2.350055000000	F	6.174115000000	2.181065000000	2.259100000000
C	1.577546000000	-1.678609000000	-2.684469000000	F	7.197301000000	0.949825000000	0.789009000000
C	1.486741000000	-0.314911000000	-3.018961000000	C	5.340950000000	-2.149300000000	-2.771312000000
H	0.519894000000	0.176512000000	-3.006398000000	F	6.089589000000	-1.930270000000	-3.880180000000
C	2.638142000000	0.417314000000	-3.282216000000	F	6.036207000000	-1.618281000000	-1.735456000000
C	3.899701000000	-0.174528000000	-3.215400000000	F	5.294847000000	-3.482780000000	-2.577345000000
H	4.796232000000	0.405891000000	-3.400258000000	C	2.548802000000	1.871783000000	-3.648576000000
C	3.977591000000	-1.529175000000	-2.895543000000	F	2.973341000000	2.088590000000	-4.917617000000
C	2.838737000000	-2.292894000000	-2.650090000000	F	1.293701000000	2.357934000000	-3.562280000000
H	2.913644000000	-3.337017000000	-2.390501000000	F	3.333154000000	2.638766000000	-2.851674000000
H	-0.411361000000	-1.697256000000	-2.198491000000	C	-1.685919000000	0.091280000000	-0.770979000000
O	2.106370000000	4.268407000000	-0.232945000000	O	-1.081960000000	1.083631000000	-1.233276000000
O	1.067925000000	-4.509261000000	-1.972240000000	O	-1.856918000000	-1.024279000000	-1.315706000000
Fe	-2.508355000000	0.125375000000	1.011362000000				
H	0.502367000000	-1.062727000000	5.518350000000				
H	-8.026211000000	-0.317095000000	1.204953000000				

References

- [1] P. Gotico et al, *Angew. Chem. Int. Ed.* **2019**, 58, 4504-4509
- [2] E. Hasegawa, T. Seida, N. Chiba, T. Takahashi, H. Ikeda, *J. Org. Chem.* **2005**, 70, 9632–9635
- [3] C. Prier, K. Rankic, D. W. C. MacMillan, *Chem. Rev* **2013**, 113, 5322-5363
- [4] M. J. Frisch, G. W. Trucks, H. B. Schlegel, G. E. Scuseria, M. A. Robb, J. R. Cheeseman, G. Scalmani, V. Barone, B. Mennucci, G. A. Petersson, *Gaussian Inc. Wallingford CT* **2009**.
- [5] C. Adamo, V. Barone, *J. Chem. Phys.* **1999**, 110, 6158–6170.
- [6] P. A. Davethu, S. P. de Visser, *J. Phys. Chem. A* **2019**, 123, 6527–6535.
- [7] P. Gotico, L. Rounpel, R. Guillot, M. Sircoglou, W. Leibl, Z. Halime, A. Aukauloo, *Angew. Chem. Int. Ed. Engl.* **2020**, 59, 22451–22455.
- [8] a) Becke, A. D. *J. Chem. Phys.* **1993**, 98, 5648–5652; b) Lee, C.; Yang, W.; Parr, R. G. *Phys. Rev. B: Condens. Matter Mater. Phys.* **1988**, 37, 785–789.
- [9] S. Grimme, S. Ehrlich and L. Goerigk, *J. Comput. Chem.*, **2011**, 32, 1456.
- [10] J. Tomasi, B. Mennucci, R. Cammi, *Chem. Rev.* **2005**, 105, 2999–3094.
- [11] P. J. Hay, W. R. Wadt, *J. Chem. Phys.* **1985**, 82, 299–310.
- [12] M. M. Francl, W. J. Pietro, W. J. Hehre, J. S. Binkley, M. S. Gordon, D. J. DeFrees, J. A. Pople, *J. Chem. Phys.* **1982**, 77, 3654–3665.
- [13] “Chemcraft - Graphical program for visualization of quantum chemistry computations,” can be found under <https://www.chemcraftprog.com/index.html>
- [14] R. R. Gagné, J. L. Allison, D. M. Ingle, *Inorg. Chem.* **1979**, 18, 2767